

Effect of oxygen content on the anomalies at successive phase transitions of $\text{La}_2\text{CuO}_{4+\delta}$ single crystal below 320 K

Jian Ding Yu, Yoshiyuki Inaguma, and Mitsuru Itoh*

Research Laboratory of Engineering Materials, Tokyo Institute of Technology, 4259 Nagatsuta, Midori-ku, Yokohama 226, Japan

Masaharu Oguni and Tôru Kyômen

Department of Chemistry, Faculty of Science, Tokyo Institute of Technology, 2-12-1 Ookayama, Meguro-ku, Tokyo 152, Japan

(Received 21 March 1996; revised manuscript received 7 May 1996)

A detailed study of electronic and thermal transport properties and linear thermal expansion of $\text{La}_2\text{CuO}_{4+\delta}$ single crystals with both high oxygen pressure oxidation and electrochemical oxidation were carried out. A series of anomalies of resistivity, thermoelectric power, and linear thermal expansion have been observed at three successive phase transitions below room temperature in samples with $0 < \delta \leq 0.035$. These anomalies are gradually depressed with $\delta > 0.035$, achieved by the electrochemical oxidation, and nearly disappear after electrochemical oxidation for 40 days. [S0163-1829(96)01234-9]

I. INTRODUCTION

Because of its simple structure and composition, extensive studies of magnetism, electronic properties, thermal transport, superconductivity, and structure have been carried out in the $\text{La}_2\text{CuO}_{4+\delta}$ compound for the purpose of revealing a common dominant mechanism in the superconductivity of high- T_c cuprate superconductors.¹⁻¹² It has been established that the superconducting state of $\text{La}_2\text{CuO}_{4+\delta}$ is related to the excess oxygen content and the structural change associated with a phase transition or phase segregation. Two techniques have been employed to induce excess oxygen into stoichiometric La_2CuO_4 . The first is high-pressure oxygen annealing at 500–600 °C, yielding $\delta \sim 0.035$, and producing a superconducting phase with $T_c \sim 35$ K.^{8,9} The second is electrochemical oxidation at room temperature, which can increase the excess oxygen up to $\delta = 0.12$ and result a T_c as high as 45 K.^{13,14}

Neutron-diffraction studies of $\text{La}_2\text{CuO}_{4+\delta}$ ($\delta \sim 0.035$) have revealed that a reversible phase segregation into two phases occurs below 300 K, an oxygen-poor phase (insulating and antiferromagnetic) and oxygen-rich phase (metallic and superconducting).⁷⁻⁹ The oxygen-poor phase has $Bmab$ symmetry and the oxygen-rich phase was considered to be $Fmmm$ symmetry by Jorgensen *et al.*⁷ and $Bmab$ symmetry by Chaillout *et al.*⁸ In their studies, a remarkable feature is that the phase segregation is reported to occur via diffusion of oxygen atoms that remain mobile down to about 200 K. Ahrens *et al.*¹⁵ have reported that a slow cooling through a narrow temperature range around 190 K made $T_c \sim 33$ K, 4 K higher than that following rapid cooling, ~ 29 K. The reason for this is interpreted as due to the reduction of excess oxygen mobility during rapid cooling and the freezing-in of the nonequilibrium state during the phase segregation process. Thus, the freezing of oxygen diffusion causes a decrease in the excess oxygen content of the metallic superconducting phase and leads to a lower T_c .

Based on our heat-capacity measurements,^{16,17} we have reported that the single crystal samples of $\text{La}_2\text{CuO}_{4+\delta}$

($0 < \delta \leq 0.035$), heat treated with different partial oxygen pressures, undergo three successive phase transitions below room temperature. We do not observe the oxygen migration in the process of successive phase transitions.¹⁶⁻¹⁹ Therefore, we propose that the phase separation associated with oxygen migration occurs at $T > 320$ K. The three successive phase transitions are concluded to be (1) a second-order phase transition, the phase transition temperature defined as T_s , (2) a martensitic-like phase transition, the phase transition temperature defined as T_m , (3) a first-order phase transition, the phase transition temperature defined as T_f . In the measurement of resistivity under hydrostatic pressure for the $\text{La}_2\text{CuO}_{4.035}$ single-crystal sample, the second-order phase transition at T_s , the martensitic-like phase transition at T_m , and the first-order phase transition at T_f are all suppressed when the hydrostatic pressure is higher than a critical value (8 kbars).¹⁸ This evidence implies that the three successive phase transitions may be related to the internal elastic stress occurring in the coexisting oxygen-poor phase and the oxygen-rich phase. It is known that $\text{La}_2\text{CuO}_{4+\delta}$ compounds have no phase separation when $\delta > 0.045$.¹³ It is worth investigating if three successive phase transitions still exist in the single phase state ($Fmmm$) when $\delta > 0.045$.

In this paper, we present first the drastic anomalies in resistivity, thermoelectric power, and thermal expansion which occur at the three successive phase transitions for samples ($0.001 \leq \delta \leq 0.035$) heat-treated with different partial oxygen pressure atmospheres. Secondly, we show the changes in these anomalies following electrochemical oxidation to $\delta > 0.035$. Finally, we try to interpret the anomalous electronic and thermal transport properties using the correlation polaron model proposed by Goodenough and co-workers.^{20,21}

II. EXPERIMENTAL

The single crystals were grown by the traveling solvent floating-zone method.²² The excess oxygen content was first changed in the range $0 < \delta \leq 0.035$ by high-temperature annealing under different partial pressures of oxygen. The ex-

cess oxygen contents were determined by iodometric titration, and the dependence of the annealing conditions on the excess oxygen content has been reported previously.¹⁹ In order to further increase oxygen content, two samples annealed under high oxygen pressure, $\text{La}_2\text{CuO}_{4.015}$ and $\text{La}_2\text{CuO}_{4.021}$, were then electrochemically oxidized. A piece of the $\text{La}_2\text{CuO}_{4.015}$ sample, with a section in perpendicular to the CuO_2 plane (dimensions of $3 \times 2 \text{ mm}^2$ and the thickness 1.5 mm), was used to measure the resistivity along the c axis ρ_{\perp} . A piece of the $\text{La}_2\text{CuO}_{4.021}$ sample, with a section parallel to the CuO_2 plane (dimensions of $4 \times 3 \text{ mm}^2$ and the thickness 1.5 mm), was used to measure the resistivity parallel to the ab plane, ρ_{\parallel} ; the Seebeck coefficient parallel to ab plane, S_{\parallel} , and along the c axis, S_{\perp} .

The electrochemical cell was set up as $\text{La}_2\text{CuO}_{4+\delta} | 1 \text{ M KOH aq} | \text{Pt}$, where the positive electrode was a single crystal of $\text{La}_2\text{CuO}_{4+\delta}$ and the negative electrode was a thin platinum plate. Pt wire with 0.1 mm diameter was soldered to a section of sample with indium, and the indium was covered completely with silicone rubber. An $\text{Ag} | \text{AgCl}$ electrode was used as a reference electrode connected to the solution via a salt bridge.²³ A constant current of $10 \mu\text{A}$ was passed through the cell. To observe the change of electronic and thermal transport properties resulting from the electrochemical oxidation, the resistivity and Seebeck coefficient were measured before and after electrochemical oxidation for 7, 20, and 40 days. The sample piece was so small that it was difficult to determine the excess oxygen content after electrochemical oxidation by the change of mass, but the change of oxygen content can be estimated from the change of the Seebeck coefficient at room temperature. Electrical resistivity was measured by a four-probe dc method in the temperature range 10–320 K. The Seebeck coefficient was measured during warming from 80 to 320 K with a homemade device. The linear thermal expansion was measured by a strain gauge method.^{24,25} A small gauge, of size $2 \times 2 \text{ mm}^2$, was attached to the sample with epoxy resin and formed a resistance bridge with another three resistors. The unbalanced voltage of the bridge resulting from temperature change is proportional to the linear thermal expansion. The resolution of the strain gauge is about 10^{-8} . The strain was calculated using the linear thermal expansion of a reference Cu sample.

III. RESULTS

The significant anomalies in resistivity (ρ) and Seebeck coefficient (S) for $\text{La}_2\text{CuO}_{4+\delta}$ ($\delta = 0.001 - 0.035$) single crystals are obtained at three phase transition temperatures, T_s , T_m and T_f . When $\delta > 0.035$, the significant anomalies are gradually suppressed with increasing δ following electrochemical oxidation.

Figures 1 and 2 show the temperature dependence of ρ_{\perp} and ρ_{\parallel} , respectively, for $\text{La}_2\text{CuO}_{4+\delta}$ ($0.001 \leq \delta \leq 0.035$) single crystals oxidized by high-temperature annealing. For ρ_{\perp} , no anomaly is observed for the $\delta = 0.001$ sample, implying that the successive phase transitions do not occur in this sample. Two anomalies are observed for the $\delta = 0.005$ sample and three anomalies are observed for the $\delta > 0.005$ samples. T_s depends on δ and increases from 255 to 298 K in the range $0.005 \leq \delta \leq 0.015$. When $\delta > 0.015$, T_s has a constant value, $T_s = 298 \text{ K}$. Hysteresis occurs around

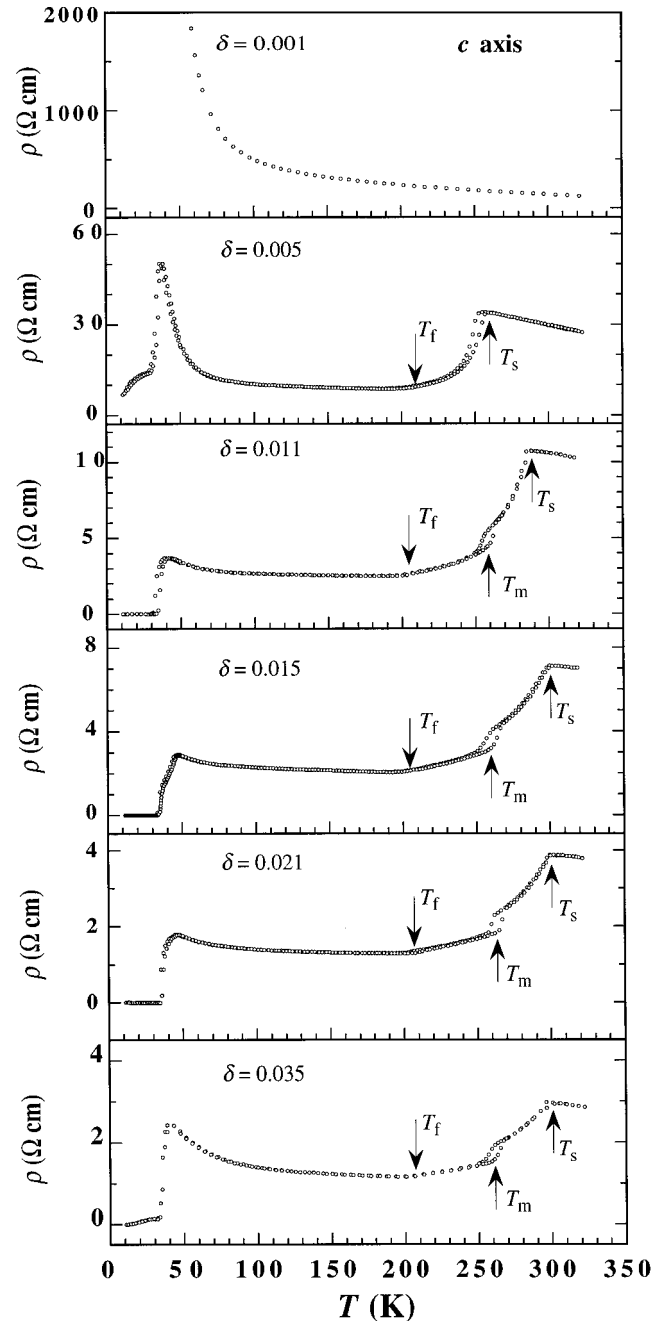


FIG. 1. Temperature dependence of resistivity along the c axis for $\text{La}_2\text{CuO}_{4+\delta}$ single crystals.

$T_m = 265 \pm 5 \text{ K}$ for the $\delta \geq 0.011$ sample. Since the $\delta = 0.005$ sample does not show such a hysteresis loop, and has a very low $T_s = 255 \text{ K}$, we conclude that the martensitic-like phase transition does not occur. When $T < T_m$, ρ_{\perp} decreases with a smaller slope and reaches a minimum value at T_f for the $\delta \geq 0.005$ samples. When $T < T_f$, ρ_{\perp} shows semiconducting behavior up to T_c . For ρ_{\parallel} , it is noted that the anomalous feature at T_s is very sensitive to δ . The decreasing slope of ρ_{\parallel} below T_s becomes smaller with increasing δ , and the anomalous feature at T_s disappears when $\delta = 0.035$, but the hysteresis loop still persists as shown in the inset. The temperature variation of ρ_{\parallel} , in the range T_s to T_f , changes from metallic behavior to semiconducting be-

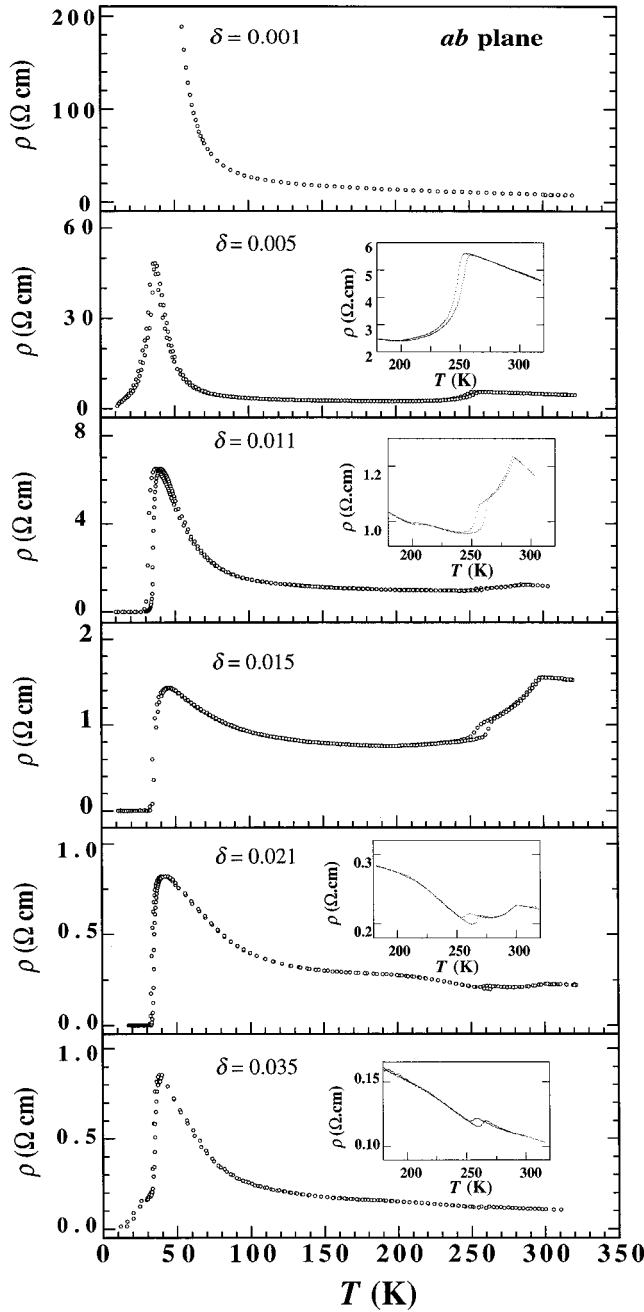


FIG. 2. Temperature dependence of resistivity along the ab plane for $\text{La}_2\text{CuO}_{4+\delta}$ single crystals.

havior when δ increases from $\delta=0.015$ to $\delta=0.035$. Superconductivity is observed for samples with $\delta \geq 0.005$. $T_{c\text{-mid}}$ defined by the temperature where sample resistivity drops to half of its value at T_{on} , is slightly increased from 32 to 35 K with increasing excess oxygen content from $\delta=0.005$ to $\delta=0.035$.

Figures 3 and 4 show the temperature dependence of the Seebeck coefficients S_{\parallel} and S_{\perp} , respectively, for $\text{La}_2\text{CuO}_{4+\delta}$ ($0.001 \leq \delta \leq 0.035$) single crystals. It is surprising to note that the anomalous features in the Seebeck coefficient at the three phase transition temperatures have nearly the same characteristics as those in the resistivity. Similar to the resistivity measurements, two anomalies are observed for

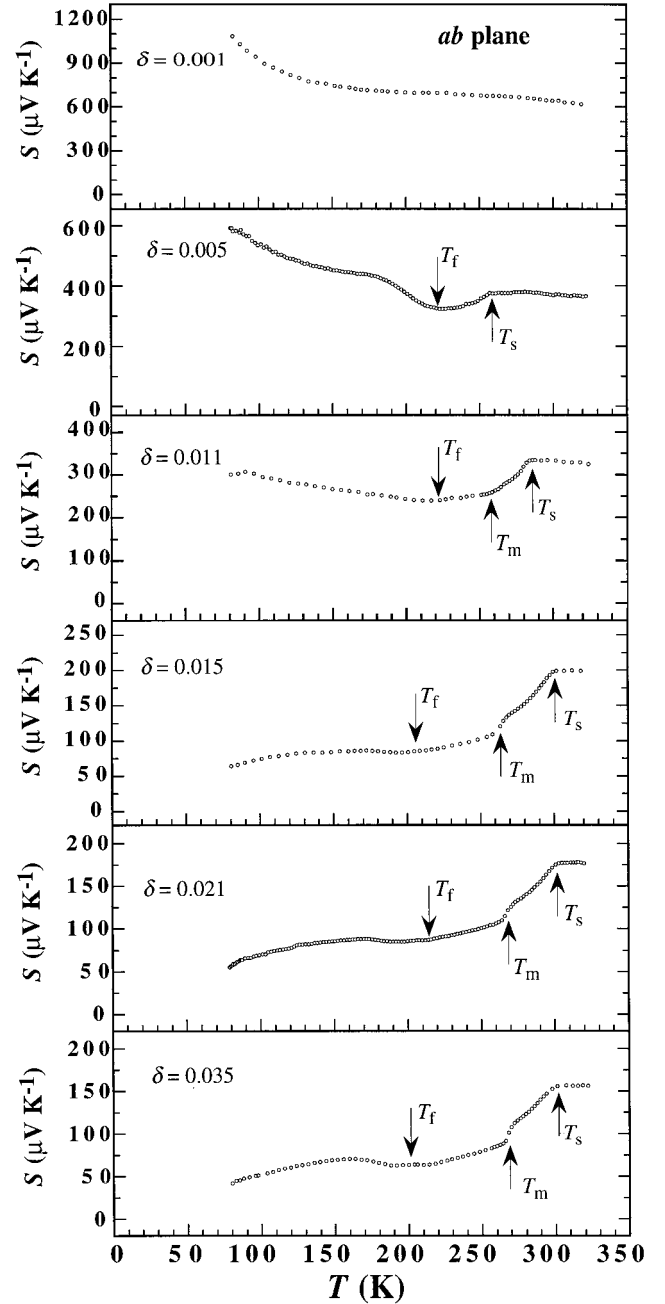


FIG. 3. Temperature dependence of Seebeck coefficient along the ab plane for $\text{La}_2\text{CuO}_{4+\delta}$ single crystals.

the $\delta=0.005$ sample, and three anomalies are observed for the $\delta > 0.005$ samples. As shown in Figs. 3, S_{\parallel} is temperature independent above T_s and drops precipitously by $\sim 60 \mu\text{V K}^{-1}$ when the temperature decreases from T_s to near T_m , with the S_{\parallel} decreases approximately by $15\text{--}20 \mu\text{V K}^{-1}$ from 270 to 265 K. A minimum value of S_{\parallel} around T_f is also observed for the samples with $\delta \geq 0.005$. In Fig. 4, we can see that the anomalous feature in S_{\perp} becomes weaker with increasing δ , and that S_{\perp} tends to decrease linearly with decreasing temperature when δ increases to 0.035.

Figure 5 shows the temperature dependence of resistivity

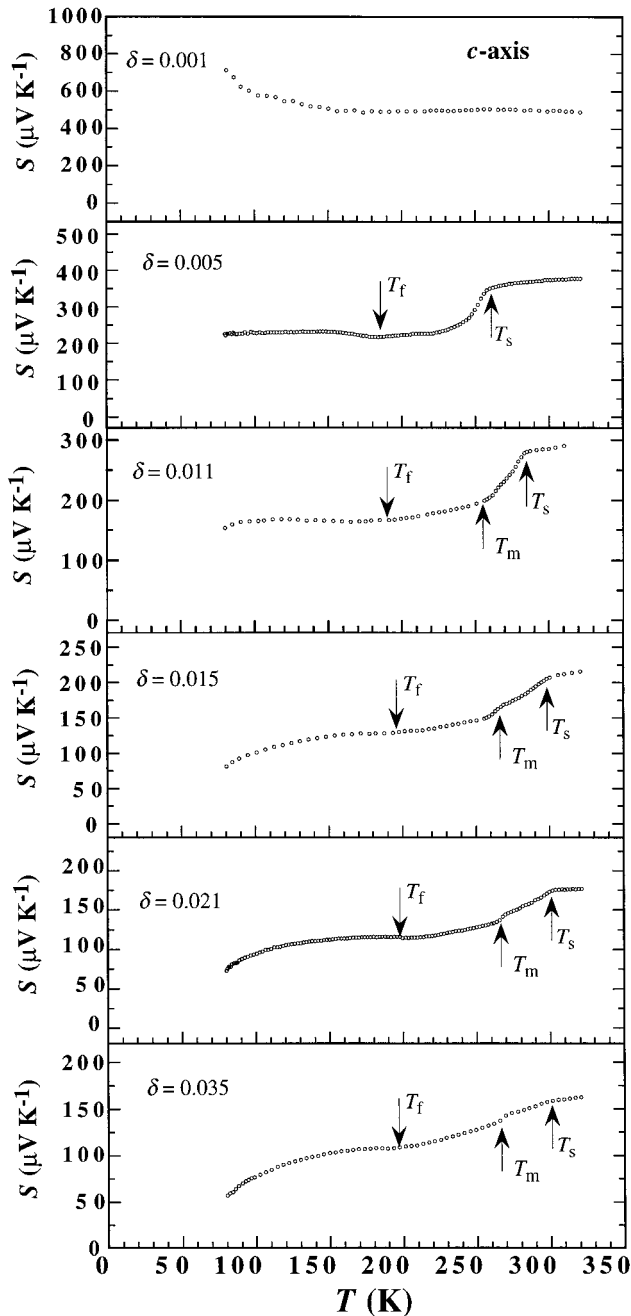


FIG. 4. Temperature dependence of Seebeck coefficient along the c axis for $\text{La}_2\text{CuO}_{4+\delta}$ single crystals.

before and after electrochemical oxidation for 20 days and 40 days for the $\text{La}_2\text{CuO}_{4.015}$ single crystal measured along the c axis [Fig. 5(a)], ρ_{\perp} and for the $\text{La}_2\text{CuO}_{4.021}$ single crystal measured along the ab plane [Fig. 5(b)], ρ_{\parallel} . The inset in Fig. 5(b) shows an expanded portion around the superconducting transition temperature. Both ρ_{\perp} and ρ_{\parallel} become nearly temperature independent from 350 K to T_c after electrochemical oxidation for 40 days. The resistivity at 300 K decreases by one half for ρ_{\parallel} and by about 20 times for ρ_{\perp} after the 40 day electrochemical oxidation. Apparently, the anomalies associated with the three phase transitions are successively suppressed with increasing electrochemical oxidation time. $T_{c\text{-mid}}$ increases to 45 K after the electrochemical oxidation for 40 days.

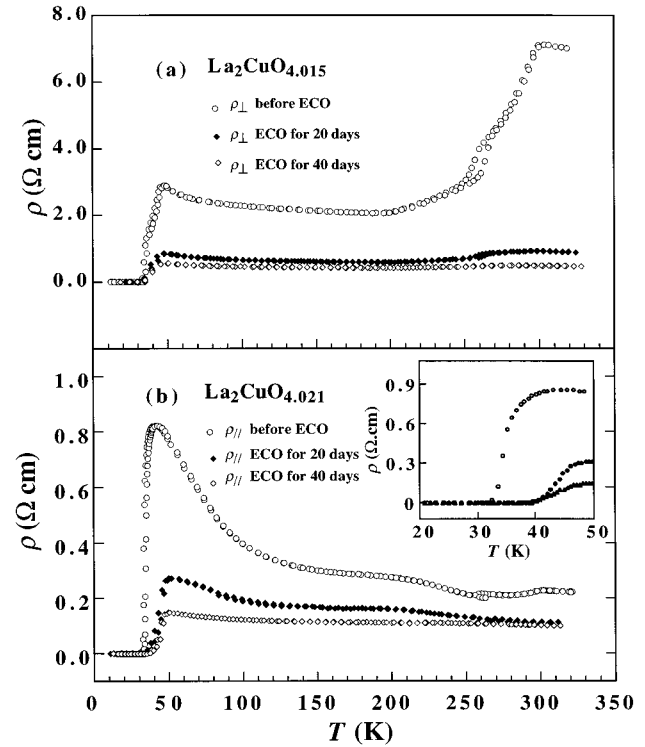


FIG. 5. The temperature dependence of resistivity before and after electrochemical oxidation for 20 days and 40 days for a $\text{La}_2\text{CuO}_{4.015}$ single crystal measured along the c axis (a) and for a $\text{La}_2\text{CuO}_{4.021}$ single crystal measured along the ab plane (b). The inset in (b) shows an expanded portion around T_c . The abbreviation ECO means electrochemical oxidation.

Figure 6 shows the temperature dependence of the Seebeck coefficient for the $\text{La}_2\text{CuO}_{4.021}$ single crystal, before and after electrochemical oxidation for 20, and 40 days measured along the ab plane [Fig. 6(a)], S_{\parallel} ; and before and after electrochemical oxidation for 40 days measured along the c axis [Fig. 6(b)], S_{\perp} . After electrochemical oxidation for 40 days, the magnitude of S_{\parallel} above T_s drops by about $100 \mu\text{V K}^{-1}$ and becomes nearly independent ($\approx 60 \mu\text{V K}^{-1}$) in the temperature range $160 \text{ K} < T < 320 \text{ K}$ in spite of a slight remaining trace of anomalies at T_m and T_f . This implies that the excess oxygen content has been significantly increased during the electrochemical oxidation process and the three phase transitions suppressed. After the electrochemical oxidation, S_{\perp} has the same magnitude as S_{\parallel} and also becomes temperature independent from 80 to 320 K.

Further information about the three anomalies is given by the linear thermal-expansion coefficient data shown in Fig. 7. We measured the linear thermal expansion along $\langle 110 \rangle$ for a $\text{La}_2\text{CuO}_{4.035}$ single crystal [Fig. 7(a)] and for an electrochemically oxidized single-crystal sample [Fig. 7(b)]. For the $\text{La}_2\text{CuO}_{4.035}$ single crystal, a very sharp peak in the linear thermal-expansion coefficient ($\Delta\alpha = 15 \times 10^{-6} \text{ K}^{-1}$) occurs at T_m as shown in the inset of Fig. 7(a). This provides direct evidence of a structural change, caused by the martensitic-like phase transition, through a cooperative displacement of atoms. A hysteresis loop from T_s to T_m is observed in the linear-expansion curve before electrochemical oxidation. For the electrochemically oxidized single crystal, no apparent

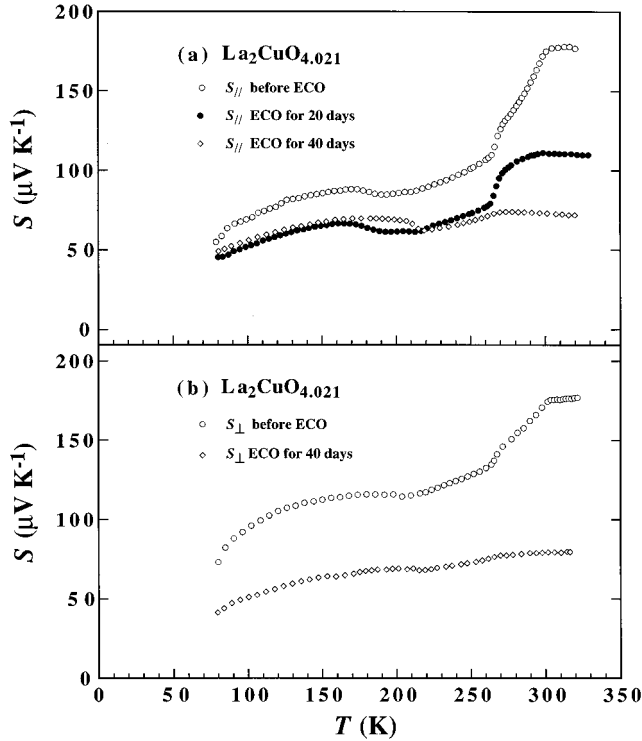


FIG. 6. The temperature dependence of the Seebeck coefficient for a $\text{La}_2\text{CuO}_{4.021}$ single crystal before and after electrochemical oxidation for 20 days and 40 days measured along the ab plane (a), and before and after electrochemical oxidation for 40 days measured along the c axis (b). The abbreviation ECO means electrochemical oxidation.

anomaly was observed. Comparing the linear thermal expansion of the samples before and after electrochemical oxidation, it is clear that the significant anomaly at T_m disappears due to an increase of the excess oxygen content.

IV. DISCUSSION

Hundley and co-workers^{6,7} have also observed the same transport anomalies found by us in both the resistivity and Seebeck coefficient at T_s for $\text{La}_2\text{CuO}_{4+\delta}$ ($\delta \leq 0.032$) single crystals. They assumed that T_s represents a phase separation temperature associated with oxygen diffusion, and the change of ρ and S from temperature independent to a linear decrease dependence can be explained by the formation of an oxygen-rich phase and an oxygen-poor phase in a phase separation. According to this interpretation, since the oxygen-rich phase exhibits metallic behavior, and because the amount of excess oxygen in the oxygen-rich phase will increase with decreasing temperature, ρ and S will linearly decrease with decreasing temperature when $T < T_s$. However, based on our heat-capacity data,^{16,17} T_s represents a second-order phase transition temperature with no oxygen diffusion, so the transport anomalies at T_s cannot be explained simply by phase separation.

We have indicated that the three successive phase transitions may be induced by internal elastic strain.¹⁸ In $\text{La}_2\text{CuO}_{4+\delta}$ compounds, two internal elastic strains can be considered. One is the local lattice distortion caused by in-

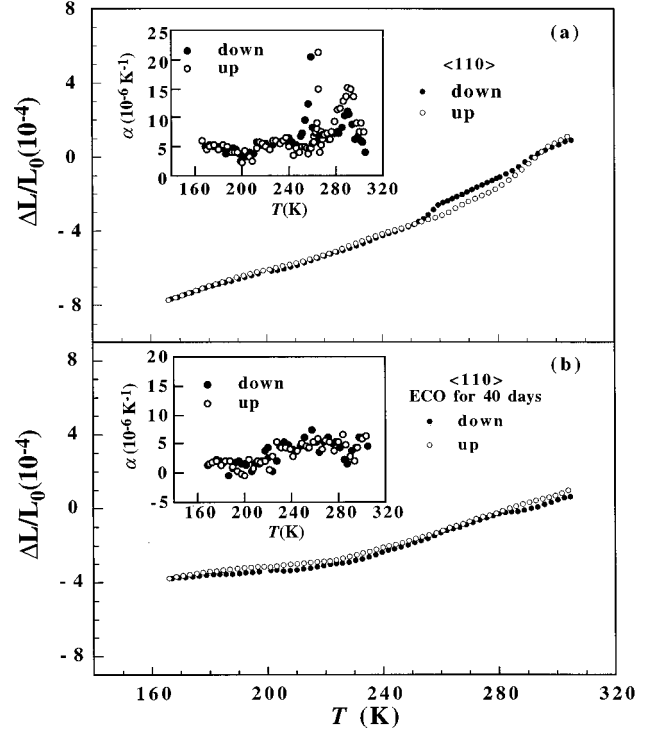


FIG. 7. Linear thermal expansion and linear thermal-expansion coefficient (in the inset) of a $\text{La}_2\text{CuO}_{4.035}$ single crystal; (a) before electrochemical oxidation, (b) after electrochemical oxidation. The abbreviation ECO means electrochemical oxidation.

terstitial oxygen ions. It will increase with increasing oxygen content. The other is caused by the bond length mismatch, which can be quantified by means of the orthorhombic strain $(b-a)/(b+a)$. In $\text{La}_2\text{CuO}_{4+\delta}$ compounds, the orthorhombic strain decreases with increasing excess oxygen content, and has a minimum value when $\delta = 0.08$.¹³ The internal elastic strain in $\text{La}_2\text{CuO}_{4+\delta}$ compounds can be attributed to the competition between the local lattice distortion and the orthorhombic strain. In the range $0.005 \leq \delta < 0.015$, the local distortion caused by the interstitial oxygen ions may be dominant. Hence, T_s increases with increasing δ . When $\delta \geq 0.015$, the two effects may compensate and T_s becomes constant. When $\delta > 0.035$, the decrease in orthorhombic strain may be larger than the local distortion and could lead to the disappearance of T_s .

The relieving of internal elastic strain due to the second-order phase transition at T_s accompanied by the change of resistivity at T_s from temperature-independent behavior to a linear temperature dependence, may be explained by the correlation polaron model proposed by Goodenough and co-workers.^{20,21} They have suggested that in cuprate superconductors the hole-rich domains have covalent Cu-O bonds and the hole-poor domains have ionic Cu-O bonds. The covalent Cu-O bonds have a shorter equilibrium length than that of ionic Cu-O bonds. They have postulated²¹ that the holes are trapped within a mobile volume of covalent Cu-O bonds embedded in a background of ionic Cu-O bonds; the mobile volume of covalent Cu-O bonds constitutes as intermediate-size polaron within which the correlation splitting energy U is sharply reduced. The mobile volume is de-

finer as a correlation polaron. The correlation polaron can move diffusively via vibronic coupling, without an associated motional enthalpy. The vibronic coupling arises from a resonance between the covalent and ionic Cu-O bonding. The two bond equilibrium energy for the resonance is considered as; $\Delta E_H = 1/2U + \Delta E_{el}$, where ΔE_H is the gain in hybridization energy, $1/2U$ is the loss of the one-side correlation splitting energy, and ΔE_{el} is the change of the elastic energy. If ΔE_{el} is very small, the correlation polaron can move by vibronic coupling and the resistivity will decrease linearly with decreasing temperature. If ΔE_{el} is not small, the correlation polaron will be trapped in and the resistivity will be nearly temperature independent. In the samples with $0 < \delta \leq 0.035$, when $T > T_s$, ΔE_{el} may not be very small and the correlation polaron cannot move diffusively by vibronic coupling. Hence, the resistivity is nearly temperature independent or shows semiconducting behavior. When $T \leq T_s$, ΔE_{el} will be reduced sufficiently by the second-order phase transition to allow the correlation polaron to move by vibronic coupling. Thus, the resistivity decreases linearly with decreasing temperature. In the samples with $\delta > 0.035$, ΔE_{el} becomes very small with increasing δ , and the second-order phase transition, and the corresponding transport anomalies, tend to disappear.

The martensitic-like phase transition also can be considered as arising from the internal elastic stress related to the tilting of the CuO_6 octahedra. It has been pointed out^{1,3} that below the orthorhombic-to-tetragonal phase transition temperature the tilting angle of the CuO_6 octahedra in oxygen-poor domains increases with decreasing temperature, but in the oxygen-rich domains the increase of tilting angle is locally disrupted due to the interstitial oxygen. The incoherence of the tilting angle in the oxygen-rich phase presumably extends to the interface between the oxygen-poor domains and the oxygen-rich domains, and forms an elastic stress in the interface. The interfacial elastic stress increases with decreasing temperature, and at T_m it becomes large enough to cause the martensitic-like phase transition through a cooperative atom displacement. In our experiments, the drastic structural change at T_m is related to the anomalies in ρ , S , and the linear expansion coefficient. We have reported that under high hydrostatic pressures T_m is initially increased and then disappears when the pressure becomes higher than a critical pressure.¹⁸ This suggests that a lower external stress will work to reduce the internal stress required to induce the transition, and that application of external pressure initially enhances the phase transition temperatures. On the other hand, above a critical pressure, the interface between the oxygen-poor domains and the oxygen-rich domains may suffer from deformation before the internal stress induces the transition, which reduces the interfacial stress and causes T_m to disappear. Furthermore, in this paper we have seen that the transport anomaly at T_m disappears after electrochemical oxidation for 40 days. This is explained because $\text{La}_2\text{CuO}_{4+\delta}$

becomes a single oxygen-rich phase ($Fmmm$) with no interfacial stress, when $\delta > 0.045$.

Below T_m an interface exists between the oxygen-poor and oxygen-rich phases, which is induced by cooperative atom displacement. Phase separation behavior can be easily observed by neutron diffraction and other methods.^{7,8,15} Since the interface formed by the martensitic-like phase transition will disrupt the polaron movement diffusively, the decreasing slopes of ρ and S become small below T_m , as shown in Figs. 1 and 4.

At T_f , a first-order phase transition occurs in the oxygen-rich phase as we have reported.¹⁷ New grains and grain boundaries will appear in the oxygen-rich phase.¹⁷ These new grains and grain boundaries may break the vibronic coupling and restrict the movement of correlated polarons. Therefore, the resistivity increases with decreasing temperature below T_f .

V. CONCLUSIONS

A series of electronic, thermal transport, and structural anomalies have been observed at three successive phase transitions below room temperature. These features in the normal-state electronic and thermal transport properties have been explained by the correlation polaron model proposed by Goodenough and co-workers.^{20,21}

In the samples with $0 < \delta \leq 0.035$, the resistivity and Seebeck coefficient changes from nearly temperature independent to a linear temperature dependence at a second-order phase transition temperature. Such a change is considered as arising from the correlation polaron movement, driven by vibronic coupling, due to the reduction of the internal elastic stress by the second-order phase transition.

At T_m , the martensitic-like phase transition temperature, a hysteresis loop in the resistivity curve, a precipitous drop ($\sim 60 \mu\text{V K}^{-1}$) in the Seebeck coefficient, and a sharp peak ($\Delta\alpha = 15 \times 10^{-6} \text{ K}^{-1}$) in the thermal-expansion coefficient are observed for the samples with $0 < \delta \leq 0.035$. We conclude that the driving force for the martensitic-like phase transition is the interfacial stress between the oxygen-poor microscopic domains and the oxygen-rich microscopic domains. Both T_s and T_m are gradually depressed with increasing δ , for δ greater than 0.035, through electrochemical oxidation, and nearly disappear after electrochemical oxidation for 40 days.

ACKNOWLEDGMENTS

The authors wish to express their thanks to Grant-in-Aid Scientific Research from Ministry of Education, Science and Culture of Japan. Also, thanks are due to Professor Tongkai Huang, Department of Physics of Shanghai University.

*Corresponding author.

¹T. Thio, T. R. Thurston, N. W. Preyer, P. J. Picone, M. A. Kastner, H. P. Jenssen, D. R. Gabbe, C. Y. Chen, R. J. Birgeneau, and Amnon Ahatony, Phys. Rev. B **38**, 905 (1988).

²T. Thio, C. Y. Chen, B. S. Freer, D. R. Gabbe, H. P. Jenssen, M.

A. Kastner, P. J. Picone, and N. W. Preyer, Phys. Rev. B **41**, 231 (1990).

³M. Oda, J. Phys. Soc. Jpn. **60**, 235 (1991).

⁴S.-W. Cheong, M. F. Hundley, J. D. Thompson, and Z. Fisk, Phys. Rev. B. **39**, 6567 (1989).

- ⁵M. F. Hundley, J. D. Thompson, S.-W. Cheong, and Z. Fisk, *Phys. Rev. B* **41**, 4062 (1990).
- ⁶M. F. Hundley, R. S. Kwok, S.-W. Cheong, J. D. Thompson, and Z. Fisk, *Physica C* **172**, 455 (1991).
- ⁷J. D. Jorgensen, B. Dabrowski, Shiyou. Pei, D. G. Hinks, and L. Soderholm, *Phys. Rev. B* **38**, 11 137 (1988).
- ⁸C. Chailout, J. Chenavas, S.-W. Cheong, Z. Fisk, M. Marezio, and J. E. Schirber, *Physica C* **170**, 87 (1990).
- ⁹P. Zolliker, D. E. Cox, J. B. Parise, E. M. McCarron III, and W. E. Farneth, *Phys. Rev. B* **42**, 6332 (1990).
- ¹⁰P. G. Radaelli, J. D. Jorgensen, R. Kled, D. A. Hunter, F. C. Chou, and D. C. Johnson, *Phys. Rev. B* **49**, 6239 (1994).
- ¹¹P. G. Radaelli, J. D. Jorgensen, A. J. Schultz, D. A. Hunter, J. L. Wagner, F. C. Chou, and D. C. Johnson, *Phys. Rev. B* **48**, 499 (1993).
- ¹²D. Vaknin, J. L. Zarestky, D. C. Johnson, J. E. Schirber, and Z. Fisk, *Phys. Rev. B* **49**, 9057 (1994).
- ¹³J.-C. Grenier, N. Lagueyte, A. Warriaux, J.-P. Doumerc. P. Dordor, J. Etourneau, and M. Pouchard, *Physica C* **202**, 209 (1992).
- ¹⁴F. C. Chou, D. C. Johnson, S.-W. Cheong, and P. C. Canfield, *Physica C* **216**, 66 (1993).
- ¹⁵E. T. Ahrens, A. P. Reyes, P. C. Hammel, J. D. Thompson, P. C. Canfield, Z. Fisk, and J. E. Schirber, *Physica C* **212**, 317 (1993).
- ¹⁶M. Itoh, M. Oguni, T. Kyômen, H. Tamura, J.-D. Yu, Y. Yanagida, Y. Inaguma, and T. Nakamura, *Solid State Commun.* **90**, 787 (1994).
- ¹⁷T. Kyômen, M. Oguni, M. Itoh, and J.-D. Yu, *Phys. Rev. B* **51**, 3181 (1995).
- ¹⁸M. Itoh, T. Huang, J.-D. Yu, Y. Inaguma, and T. Nakamura, *Phys. Rev. B* **51**, 1286 (1995).
- ¹⁹J.-D. Yu, M. Itoh, Y. Inaguma, and T. Nakamura, *Phys. C* **235**, 1323 (1994).
- ²⁰J. B. Goodenough, J.-S. Zhou, and J. Chan, *Phys. Rev. B* **47**, 5275 (1993).
- ²¹J. B. Goodenough and J.-S. Zhou, *Phys. Rev. B* **49**, 4251 (1994).
- ²²J.-D. Yu, Y. Yanagida, H. Takashima, Y. Inaguma, M. Itoh, and T. Nakamura, *Physica C* **209**, 442 (1993).
- ²³M. Itoh, Y.-J. Shan, S. Sakamoto, Y. Inaguma, and T. Nakamura, *Physica C* **223**, 75 (1994).
- ²⁴Y. Maeno, S. Nakayama, M. Irie, Y. Tanaka, S. Nishizaki, M. Nohara, Y. Omori, Y. Kitana, and T. Fujita, *Advances in Superconductivity VI* (Springer-Verlag, Tokyo, 1994), p. 103.
- ²⁵S. Nakayama, Y. Maeno, M. Irie, M. Nohara, F. Nakamura, and T. Fujita, *Physica C* **234**, 1283 (1994).